

We are IntechOpen, the world's leading publisher of Open Access books Built by scientists, for scientists

6,900

Open access books available

185,000

International authors and editors

200M

Downloads

Our authors are among the

154

Countries delivered to

TOP 1%

most cited scientists

12.2%

Contributors from top 500 universities



WEB OF SCIENCE™

Selection of our books indexed in the Book Citation Index
in Web of Science™ Core Collection (BKCI)

Interested in publishing with us?
Contact book.department@intechopen.com

Numbers displayed above are based on latest data collected.
For more information visit www.intechopen.com



Solar Wind: Origin, Properties and Impact on Earth

U.L. Visakh Kumar ¹ and P.J. Kurian²
*Physics Research Centre, St. Berchmans' College,
 Chanaganacherry, Kerala
 India*

1. Introduction

In visible light, the sun appears as an isolated and perfectly shaped, disc like object in the sky. In the deepest interior of the sun hydrogen nuclei steadily fuse together to form helium nucleus and thereby release large amounts of heat that slowly leak in to the solar surface. The temperature of the dense core of the sun is a few million degrees. Towards the solar surface, the temperature gradually decreases and until it reaches its minimum value of about 4300 K. The sun and all other stars consist of plasma :the gas is so hot ,that it is ionized such that it can easily conduct electric currents and generate and carry magnetic fields. The outer solar atmosphere contains several distinct layers with qualitatively different properties. The photosphere ($T \approx 6000$ K) marks the boundary between the convection zone below and the chromosphere which is surrounded by corona.

When the intense light of the solar disk is shielded during the eclipse of the sun, a faint halo with a thread like structure and a form that is reminiscent of a crown becomes visible to the naked eye. This so called corona appears to extend into space over many solar radii. A rapid transition to the hot corona occurs approximately $0.003 R_0$ above the photosphere where R_0 is the solar radius. The solar corona consists of tenuous plasma that is highly structured by the strong magnetic field that finds its origin in the solar interior. From the corona coronal emission occurs due to highly ionized ions. This lead to the conclusion that the coronal plasma must be extremely hot ; for iron to be so highly ionized, the temperature of the ambient plasma must be a few million degrees.

The coronal temperature ($T \geq 10^6$ K) thus turned out to be exceeding the photospheric temperature by almost a factor thousand. This indicates the presence of a physical process that actively heats the solar corona. The flow of energy through the solar atmosphere and the heating of the Sun's outer regions are still not fully understood. Apart from the magnetically closed coronal regions, part of the solar corona consist of open regions, above a height of $0.1 R_0$ where the magnetic field lines are not reentrant on the solar surface, but extend in to space.

The temperature of the coronal holes is one or two million degrees and this remains so over many solar radii into space so that the plasma is accelerated and escapes from the gravitational field of the sun to form the solar wind with an average flow velocity of

400km/s at 1 AU, the earth-sun distance. The entire system of sun, corona and solar wind constitutes the heliosphere, where the planets with their own magnetic fields appear as small islands in the stream.

2. Origin of solar wind

The basic types of solar wind are closely associated with the structure and the activity of the coronal magnetic field that changes over the solar cycle. The most fundamental aspect related to the magnetic field in the Sun is the working of the solar dynamo in the convection zone below the photosphere. It generates the magnetic field we observe on the solar surface including the corona. The corona is highly structured by the magnetic field of the sun. The base of the corona is a continually replenished ensemble of closed magnetic loops and open flux tubes, but above a height of $0.1R_0$, the open field lines begin to dominate. As the result of varying boundary conditions in the corona, three basic types of solar wind occur: Fast streams from large coronal holes (CHs); slow streams from small CHs and active regions (ARs), and from the boundary layers of coronal streamers; and the variable transient flows such as coronal mass ejections (CMEs), often associated with eruptive prominences, or plasmoids stemming from the top of streamers, and other ejections from ARs driven through magnetic flux emergence and reconnection (Marsch, 2006).

The steady solar wind consists of two major components: fast, tenuous, and uniform flows from large CHs, and slow, dense, and variable flows from small CHs, (Arge *et al.*, 2003) often from near the boundaries between closed and open coronal fields. The origin of fast streams seems clear, but the sources of the slow solar wind remain less obvious. The helium abundance is 3.6% in high speed wind very constant in time and almost identical for all streams. Whereas in slow wind the abundance is only 2.5% and is highly variable. The angular momentum carried away by the solar wind from the rotating sun is almost completely contained in the solar flow. This indicates that the fast wind starts from regions close to the solar rotation axis, while the slow wind is released only beyond $30 R_0$.

CME's from the Sun are spontaneous expulsions of $\approx 10^6$ K blobs of coronal plasma which carries up to ten billions of kilograms of mass, ejected at speeds ranging from a few hundred km/s to as much as 2000 km/s. Concerning their occurrence rate, the CMEs tend to accumulate around maximum solar activity, when the corona is highly magnetically structured and of multi-polar nature. The constraints on the plasma are even more extreme for a transient CME than for a steady solar wind stream, as the CME plasma density is often much higher, and its flow speed may easily reach a multiple of the average solar-wind speed (Marsch, 2006). Lusamma Joseph & P J Kurian (2010) finds elliptical distribution of CME speeds which indicates that magnetic field has a greater role in the dynamics of CME.

2.1 Solar wind from funnels in coronal holes

The coronal funnels are expanding magnetic field structures rooted in the magnetic network lanes. Using images and Doppler maps from the Solar Ultra Violet measurements of Emitted Radiation (SUMER) spectrometer and magnetograms delivered by the Michelson Doppler Imager (MDI) on the Space based solar and Heliospheric Observatory (SOHO) of ESA and NASA, a Chinese-German team of scientists have observed solar wind flows coming from funnel shaped magnetic fields which are anchored in the lanes of the magnetic network near

the surface of the Sun. The fast solar wind seems to originate in coronal funnels with a flow speed of about 10 km/s at a height of 20,000 km above the photosphere(Tu *et al.*, 2005).

Just below the surface of the sun, there are large convection cells which are associated with magnetic fields. By magnetoconvection, they become concentrated in the network lanes, where the funnel necks are anchored. The plasma, while still being confined in small loops, is brought by convection to the funnels and released there, like a bucket of water is emptied into an open water channel. For CH of the period of *Skylab* observations of the Sun (February 1973 – March 1974) it was demonstrated that there was rather strong positive correlation between the area S_{CH} of a coronal hole recorded in the X-ray range of coronal emission and maximum velocity V_M (at the Earth's orbit) of the fast solar wind stream flowing out of it(Nolte, J. T *et al.*, 1976).

2.2 Solar wind from active regions

The ARs near solar maximum were clearly identified as the source regions of slow solar wind. For example, Liewer *et al.* (2003) investigated the magnetic topology of several ARs in connection with EUV and X-ray images. Synoptic coronal maps were employed for mapping the inferred sources of the solar wind from the magnetic source surface down to the photosphere. In most cases, a dark lane, as it is familiar for the small CHs, was seen in the EUV images, thus suggesting an open magnetic field. The in-situ composition data of the solar wind associated with these regions indicates high freezing-in temperatures of the heavy ions, a result that is consistent with the inference that the AR indeed is a genuine source of the solar wind.

3. Coronal heating and acceleration of solar wind

There is heating everywhere above the solar photosphere. Chromospheric heating occurs immediately above the photosphere where the plasma is mostly neutral. The plasma density is high enough for many collisions to occur. Thus, non magnetic mechanisms such as acoustic wave dissipation tend to be considered as the dominant source of energy deposition (Narain and Ulmschneider, 1990) but magnetic effects still may be important (Goodman, 2000).

Base coronal heating “turns on” abruptly about $0.003 R_0$ above the photosphere and seems to extend out several tenths of a solar radius. Parker(1991)discussed the separation of heating mechanisms between the coronal base ($r \approx 1-1.5 R_0$) and extended radial distances beyond the sonic point ($r \approx 2-5 R_0$). In the coronal base there exists strong downward heat conduction generated by the sharp temperature gradient. The continually replenished “junkyard” of closed loops and open funnels at the coronal base (Dowdy *et al.*, 1986) evolves into a relatively uniform flux expansion in the extended corona. In this region, the magnetic energy is probably dissipated as heat by Coulomb collisions (via, e. g., viscosity, thermal conductivity, ion-neutral friction, or electrical resistivity).

Extended corona is the region where the primary solar wind acceleration occurs. The vast majority of proposed physical processes involve the transfer of energy from propagating magnetic fluctuations(waves, shocks, or turbulence to the particles.)The ultimate source of energy must be solar in origin, and thus it must somehow propagate out to the distances where the heating occurs(Tu and Marsch, 1995). At distances greater than 2 to 3 R_0 , the

proton temperature gradient is noticeably shallower than that expected from pure adiabatic expansion (Barnes *et al.*, 1995), indicating gradual heating of the collisionless plasma.

Near the distant termination shock, where the solar wind meets the interstellar medium, heating may occur when neutral interstellar atoms enter the heliosphere and become ionized, forming a beam or ring-like velocity distribution that is unstable to the generation of MHD waves (Zank *et al.*, 1999).

The dual questions of how the solar corona is heated and how the solar wind expands and accelerates have been considered together primarily by Hollweg (Hollweg 1986; Hollweg & Johnson 1988) since the solar wind is an outward extension of the corona. Thus, it is at least possible that similar physical processes are at work in both regions. Various mechanisms have been proposed in an effort to understand the heating of the solar corona and the acceleration of the solar wind. Unfortunately, there is no consensus among researchers about the physical mechanism(s) for coronal heating and for solar wind acceleration, even today.

The first calculation yielding a supersonic wind was performed by Parker in 1958 and was soon confirmed by in situ observations. The flow energy for the solar wind must come ultimately from what is provided at the base of the wind, where the flow speed is very small. Hence the asymptotic flow speed V_{sw} , at a very large distance where the flow kinetic energy dominates all other forms of energy, is constrained by the energy available as

$$\frac{V_{sw}^2}{2} \approx \frac{5K_B T_0}{m_p} - \frac{M_0 G}{r_0} + \frac{Q_0}{n_0 m_p V_0} \quad (1)$$

The terms on the right-hand side of (1) are respectively:

- the enthalpy per unit mass, due to both the protons and the electrons,
- the gravitational binding energy per unit mass,
- the heat flux per unit mass flux,

At the base of the wind; the initial bulk kinetic energy has been neglected, as well as the asymptotic enthalpy and heat flux terms. With a coronal temperature of 2×10^6 K, the radius $r_0 \approx 7 \times 10^8$ m, and the solar mass $M_0 \approx 2 \times 10^{30}$ kg, the enthalpy provides only 0.8×10^{11} J kg⁻¹, whereas the gravitational binding energy amounts to 2×10^{11} J kg⁻¹. Hence the available enthalpy is far from sufficient to lift the medium out of the Sun's gravitational well, so that the heat flux plays a key role. The heat is transported by the electrons, since they have a much greater thermal speed than the protons. With a coronal temperature of 2×10^6 K, the heat flux at the base of the wind provides about 2×10^{11} J kg⁻¹, which just balances the binding gravitational energy. The remaining enthalpy term yields a terminal velocity of a few hundred km s⁻¹, so that enough energy seems available to drive the wind. This result, however, is very sensitive to the temperature since the heat flux varies as $T^{7/2}$: with a temperature only 15% smaller, the right-hand side of (1) becomes negative.

Besides this, the wind which is the most stable, is the fastest and fills most of the heliosphere, comes from the coldest regions of the corona, where the electron thermal temperature (which determines the conductivity) is not significantly higher than 10^6 K. With such a temperature, the thermal conductivity falls short by roughly one order of magnitude of that required to drive even a low-speed wind. Hence the electron driven models were soon recognized to be insufficient to drive the high speed streams.

In 1942, by studying the mutual interaction between conducting fluid motion and electromagnetic fields Hannes Alfvén discovered a new mode of waves, that later on were named as Alfvén waves. An Alfvén wave propagating in a plasma is a traveling oscillation of the ions and the magnetic field. The ion mass density provides the inertia and the magnetic field line tension provides the restoring force. The wave vector can either propagate in the parallel direction of the magnetic field or at oblique incidence. The waves efficiently carry energy and momentum along the magnetic field lines. The Alfvén waves were identified in the solar wind by means of spacecraft measurements in late 60's. An early mention of the radiation pressure of Alfvén waves can be found in Bretherton & Garrett (1969).

Alazraki & Couturier (1971) and Belcher (1971) inaugurated the concept of the wave-driven wind by noting that the waves exert a 'wave pressure' $-\nabla\langle\delta B^2\rangle/8\pi$ on the wind where B is magnetic field, the prefix δ denotes a fluctuation, and the angle brackets denote a time-average.

Alfvén waves can travel a long distance to contribute not only to coronal heating but to the solar wind acceleration. The Alfvén waves are excited by steady transverse motions of the field lines of the photosphere while they can also be produced by continual reconnection above the photosphere. Tomczyk et al. (2007) reported the detection of Alfvén waves in images of the solar corona with the Coronal Multi-Channel Polarimeter instrument at the National Solar Observatory, New Mexico.

With heating and wave pressure, the wave-driven models were able to explain the high-speeds and hot protons observed in the fast wind in interplanetary space (e. g. , Hollweg 1978). These wave-driven models generally succeeded in explaining solar wind data far from the Sun, but they failed close to the Sun. The spacecraft gave us new coronal hole density data, which verified previous evidence that the density declines very rapidly with increasing r (Guhathakurta & Holzer 1994, Guhathakurta & Fisher 1998). That requires the flow speed to increase very rapidly with r . The wave-driven models could not achieve such rapid accelerations. The reason is simply that, close to the Sun, the wave pressure is small compared to other terms in the momentum balance.

The Ultraviolet Coronagraph Spectrometer (UVCS) aboard the *Solar and Heliospheric Observatory* (SOHO), launched in 1995, has been the first space borne instrument able to constrain ion temperature anisotropies and differential outflow speeds in the acceleration region of the wind. UVCS measured O^{5+} perpendicular temperatures exceeding 3×10^8 K at a height of $2 R_{\odot}$. Temperatures for both O^{5+} and Mg^{9+} are significantly greater than mass-proportional when compared to hydrogen, and outflow speeds for O^{5+} may exceed those of hydrogen by as much as a factor of two. These results are similar in character to the *in situ* data, but they imply more extreme departures from thermodynamic equilibrium in the corona.

Because of the perpendicular nature of the heating, and because of the velocity distribution anisotropies for positive ions in the coronal holes, UVCS observations have led to a resurgence of interest in models of coronal ion cyclotron resonance. Wave-particle interactions, such as ion-cyclotron resonance, are considered now as the principal mechanism for heating of coronal holes, and ultimately driving the fast solar wind (Hollweg 2006; Cranmer 2002, 2004). The current understanding is that the solar wind is mainly driven by the pressure of hot protons, so the heating in coronal holes goes more into protons

than electrons, because it is conveyed by the ion-cyclotron resonance rather than by currents, which is different from the DC heating models generally applied in the lower corona. By the late 1970s, various data were suggesting the importance of the ion-cyclotron resonance far from the Sun. But we still do not know the exact source of the high-frequency resonant waves (Hollweg, 2006).

Ion cyclotron waves (ICWs) are left-hand circularly polarized waves. They have been observed in a variety of space environments, including those upstream of and those within planetary magnetospheres (e. g. , Russell & Blanco-Cano 2007). These waves are often caused by newly created ions, accelerated by the electric field of a magnetized plasma flowing through a neutral gas from which the ions were produced (Gary, 1991; Huddleston & Johnstone, 1992).

Tomczyk *et al.* (2007) detected Alfvén waves by using Coronal Multi-Channel Polarimeter (CoMP) at the National Solar Observatory, New Mexico. Observations showed the existence of upward propagating waves with phase velocity $1-4 \times 10^6$ m/s. They concluded that the waves are too weak to heat the solar corona and added that the unresolved Alfvén waves may carry enough energy to heat the corona.

Recent reports have claimed that the Alfvén waves observed in the low solar atmosphere can provide an energy flux sufficient to heat the corona (De Pontieu, 2007; Jess *et al.* , 2009), but Alfvén waves, which are linearly polarized waves at a much lower frequency than ion gyrofrequencies, do not directly interact with the core ions. They need an intermediary process to convert this energy flux to a form that can heat the coronal ions efficiently. One possible energy transfer is the production and subsequent damping of ICWs (e. g. , Cranmer, 2000, 2004; Cowee *et al.* , 2007; Hollweg, 2008). The parallel wave numbers of the global resonant MHD mode are too low to directly provide ion heating through collisionless damping. At the same time, the global mode is characterized by small perpendicular length scales and thus by relatively strong currents, which can excite the ion cyclotron waves (Markvoskii, 2001).

Energy flux density of the ICW is given as (e. g. , Banerjee *et al.* , 1998),

$$F_W = \sqrt{\frac{\rho}{4\pi}} \langle \delta v^2 \rangle B \quad \text{erg cm}^{-2} \text{ s}^{-1} \quad (2)$$

The wave amplitude at heights 120" off the solar limb is about, $\langle \delta V^2 \rangle = 2 \times (43.9 \text{ kms}^{-1})^2$. Adopting the values for $B = 5 \text{ G}$ and $N_e = 4.8 \times 10^{13} \text{ m}^{-3}$ at $r = 1.25 R_0$, Banerjee *et al.* (1998) found the wave flux density as $F_W = 4.9 \times 10^5 \text{ erg cm}^{-2} \text{ s}^{-1}$ which is high enough for the ion cyclotron resonance (ICR) process to be a good candidate for heating the coronal hole.

Less understood is the mechanism of the generation of the ion cyclotron waves in coronal holes. Generation of resonant ICW may be possible by stochastic magnetic foot point motions, magnetic reconnections and MHD filamentation instabilities or from MHD turbulent cascade. This latter mechanism is supposed to be the dominant one producing ICW that heat the coronal hole plasma and accelerate the solar wind particles (Cranmer, 2000). It is possible that waves with higher frequencies and wave numbers occur throughout the corona because of a turbulent cascade starting from MHD scales (Hollweg 1986; Hollweg & Johnson 1988).

The ion cyclotron waves are generated by a plasma microinstability that is driven by current fluctuations of lower frequency MHD waves. The current required to excite the instability is consistent with the spatial scales suggested by the observations and reasonably large magnetic field fluctuations. (Markvoskii, 2001 & Vinas, Wong, & Klimas, 2000). According to another scenario, ion cyclotron waves are launched at the coronal base by reconnection events (Axford & McKenzie, 1992, Tu & Marsch, 1997).

Although ICWs cannot be remotely observed in the corona, the Solar and Heliospheric Observatory (SOHO) observations of ultraviolet emissions have been used to infer the presence of highly anisotropic heavy-ion distributions with strong mass dependent heating in the corona (e. g. , Kohl J. L. 1998; Cranmer S. R. 1999; Antonucci *et al.* , 2000). The data from STEREO A (2007 July 26–August 2) and STEREO B (2007 July 25–August 1) revealed that 246 ICW events appear discretely in the solar wind with variable durations. Unlike Alfvén turbulence that often appears in the fast wind, or the whistler waves and mirror-mode waves ICWs were not generated by shocks and they are more often when the interplanetary magnetic field (IMF) is nearly radial (Jian. K, L. *et al.* , 2009).

It is well established that the ion cyclotron waves can provide ion heating and acceleration in good agreement with the observations such as ion temperature anisotropy (Marsch 1991; Kohl J, L. , 1998), faster outflow of heavier ions (Li *et al.* 1998; Cranmer S, R. , 1999), and higher temperatures of heavy ions compared to protons (Neugebauer 1981, 1992; Kohl J, L. , 1998, 1999). However many discrepancies have to be solved in the scenario of ICW heating mechanism in lower solar corona. Even though this mechanism is found successful in heavy ions , a model for proton cyclotron resonance heating in the lower corona needs to be proposed and verified.

4. Solar wind parameters near 1 AU and their interdependence

Solar wind, usually originating from the lower corona of the Sun, travels outwards through the heliosphere. Beyond the Alfvén critical layer of about $10 R_0$, the solar wind flows with an approximate terminal velocity up to 1AU. The bulk expansion of solar wind continues to accelerate until it is beyond around $8 R_0$ and the acceleration is virtually completed by $10 R_0$ (Böhmer- Vitense, 1989). SOHO and interplanetary scintillation results show that the fast wind reaches its terminal speed by $10 R_0$, and has already been accelerated. VLBA and EISCAT measurements show that solar wind velocity reaches a maximum value at about $10 R_0$ and it attains a terminal velocity at $10 R_0$ (Harmon *et al.* , 2005). However, the solar wind turbulence plays a major role in the post critical journey of the solar wind.

As the solar wind moves outwards, velocity and temperature remain coherent, whereas density does not (Richardson, 1996). Various parameters, such as solar wind velocity, proton density, proton temperature and mean magnetic field, fluctuate in this scenario.

The interdependence among the solar wind parameters, namely solar wind velocity, proton temperature, proton density and mean magnetic field in the solar wind has been explained by a Multiple Linear Regression (MLR) model (Shollykutty John and P. J. Kurian¹, 2009) . The model was proposed for the prediction of the solar wind velocity (response variable) based on the explanatory variables proton density, proton temperature and mean magnetic field in the solar wind, collected from the ACE satellite data during January 1998 – May 2006.

Solar wind velocity is the combined effect of the inertial uniform speed along with electron plasma wave velocity which is manifested by Langmuir waves, thermal velocity represented by ion acoustic waves and the Alfvén velocity due to magnetic field.

$$V_{SW} = V_0 + \sqrt{\frac{4\pi}{k^2 n} \frac{e^2}{m_e} n(t)} + \sqrt{\frac{\gamma}{M} \frac{K}{T_0} T(t)} + \frac{B(t)}{\sqrt{4\pi p}} \tag{3}$$

where V_0 is the uniform speed due to inertia, k is the wave vector, n is the number density, B is the mean magnetic field, T is the ion temperature, K is the Boltzmann constant and M is the proton mass. The proposed MLR model is,

$$Y = \beta_0 + \beta_1 X_1 + \beta_2 X_2 + \beta_3 X_3$$

The consolidated data was fitted as,

$$V_{SW}(t) = 354.907 + 0.0216 X_1(t) + 0.00117 X_2(t) - 2.3925 X_3(t) \tag{4}$$

The driving potential in the solar wind can be expressed as ,

$$\phi = \phi_0 \exp\left(\frac{-x}{\lambda_D}\right) + K(T_e + \gamma T_i) - \left(\frac{B^2}{8\pi}\right) \tag{5}$$

The analysis revealed that the velocity and temperature are coherent in all cases, and the effect of temperature on velocity is also statistically significant. However, the proton density has an adverse effect on the solar wind velocity in major cases for the respective period.

There exists non-linear relationship between solar wind velocity and proton density and the variation is in an inverse manner (Fig 1). Solar wind speed increases with proton temperature and the relation is linear(Fig 2). The relation between solar wind velocity and

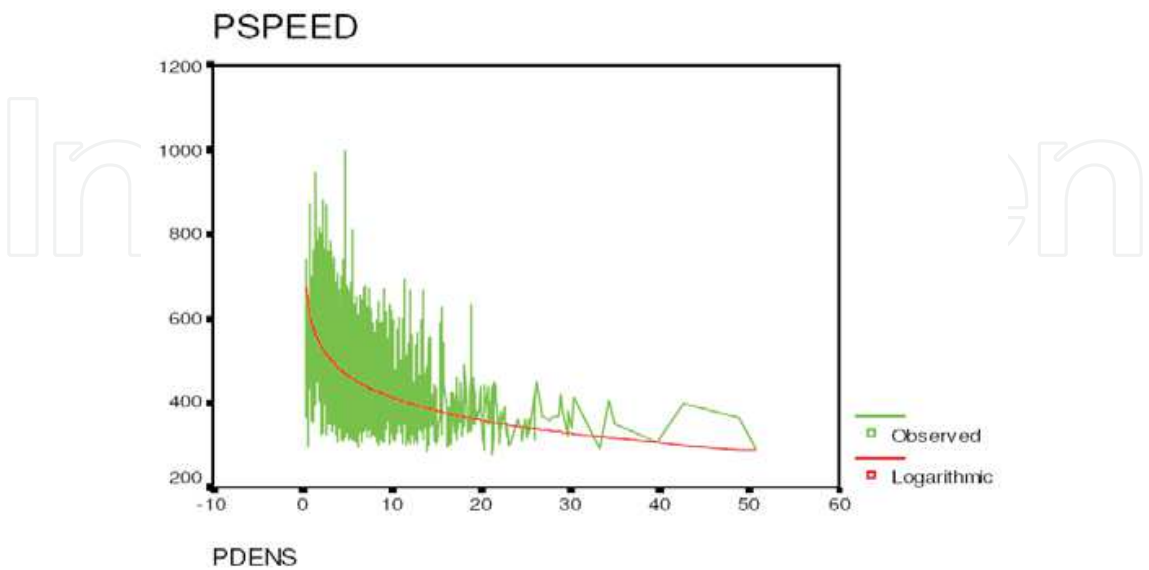


Fig. 1. Variation of solar wind proton speed (velocity) with proton density (for observed and fitted values). The abscissa is in cm⁻³ and the ordinate is in km s⁻¹.

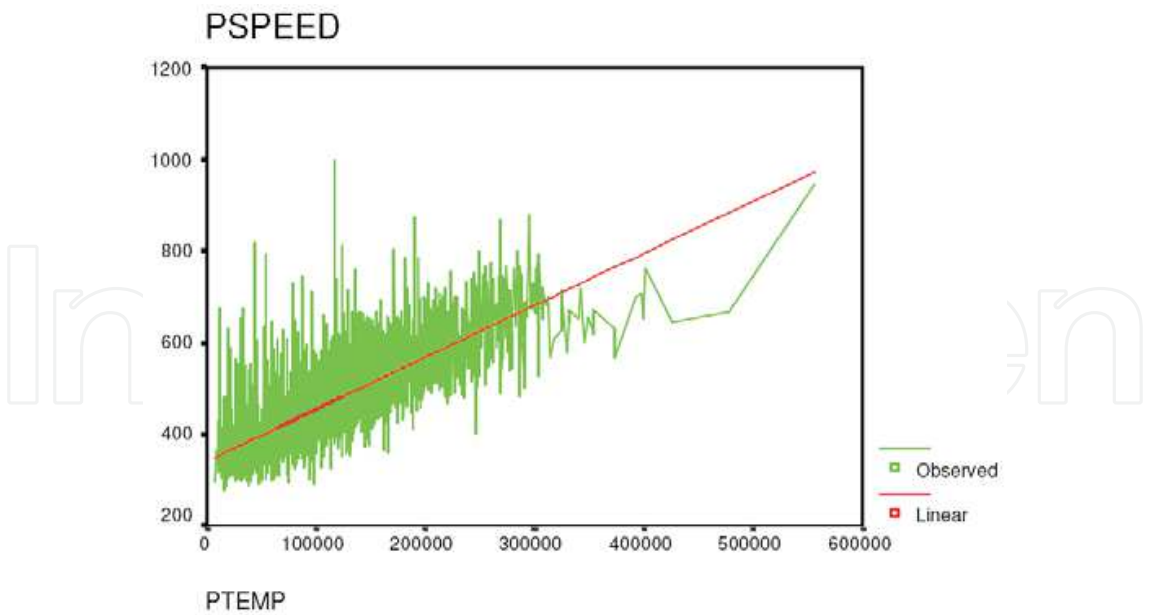


Fig. 2. Variation of solar wind proton speed (velocity) with proton temperature (for observed and fitted values). The abscissa is in Kelvin and ordinate is in km s⁻¹.

magnetic field is also non linear(Fig 3). Hence the study reveals that there is a significant correlation between solar wind velocity with the parameters proton density, proton temperature and average magnetic field in the solar wind.

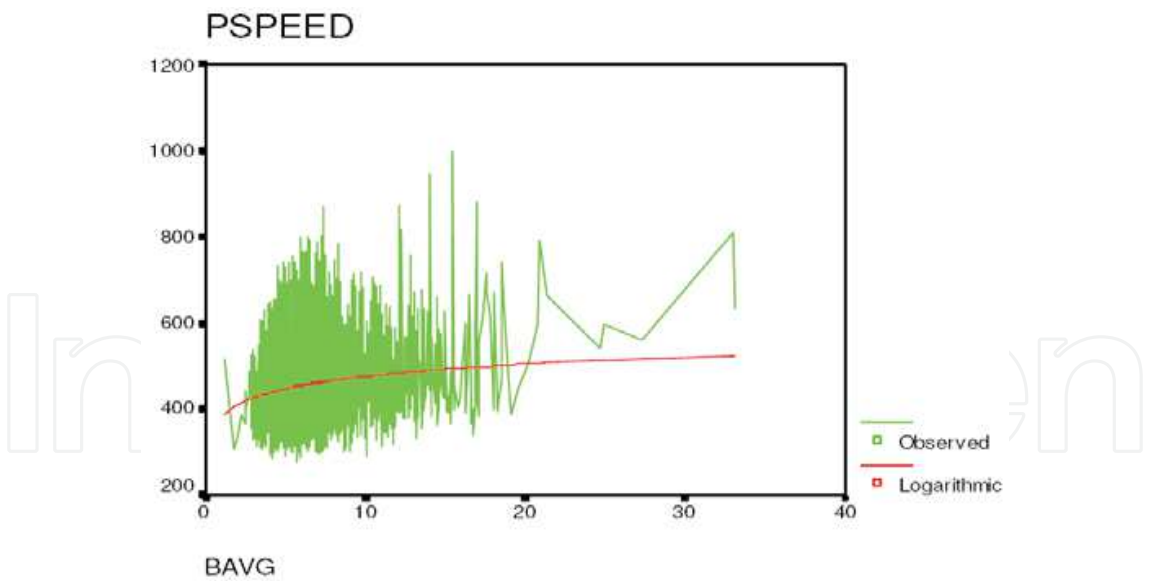


Fig. 3. Variation of solar wind proton speed (velocity) with *B* avg. (for observed and fitted values). The abscissa is in nano Tesla and the ordinate is in km s⁻¹.

Burlaga,L. F. ,(1993) has done a detailed analysis of the solar wind data obtained from various spacecrafts and he found some signatures of chaos (multifractals, intermittence and turbulence) in the solar wind. Buti (1996) showed that the chaotic fields generated in the solar wind can lead to anomalously large plasma heating and acceleration.

Shollykutty John&P. J Kurian²(2009)proved the existence of deterministic chaos in the solar wind flow by analyzing the solar wind data of daily average values of solar wind velocity, density and temperature from January 1998 to October 2006 from ACE spacecraft measured *in situ* in the heliosphere at 1 AU using techniques of time series analysis. After calculating the natural logarithm of the correlation sum $C_m(\epsilon)$ vs. $\ln \epsilon$ for various embedding dimensions, they plot the slope of the curves for various embedding dimensions as in figures 4 a-c. The slope for which saturation occurs is the correlation dimension D_2 of the attractor. The attractor dimension for the velocity profile was 7. 84 bits/ and the

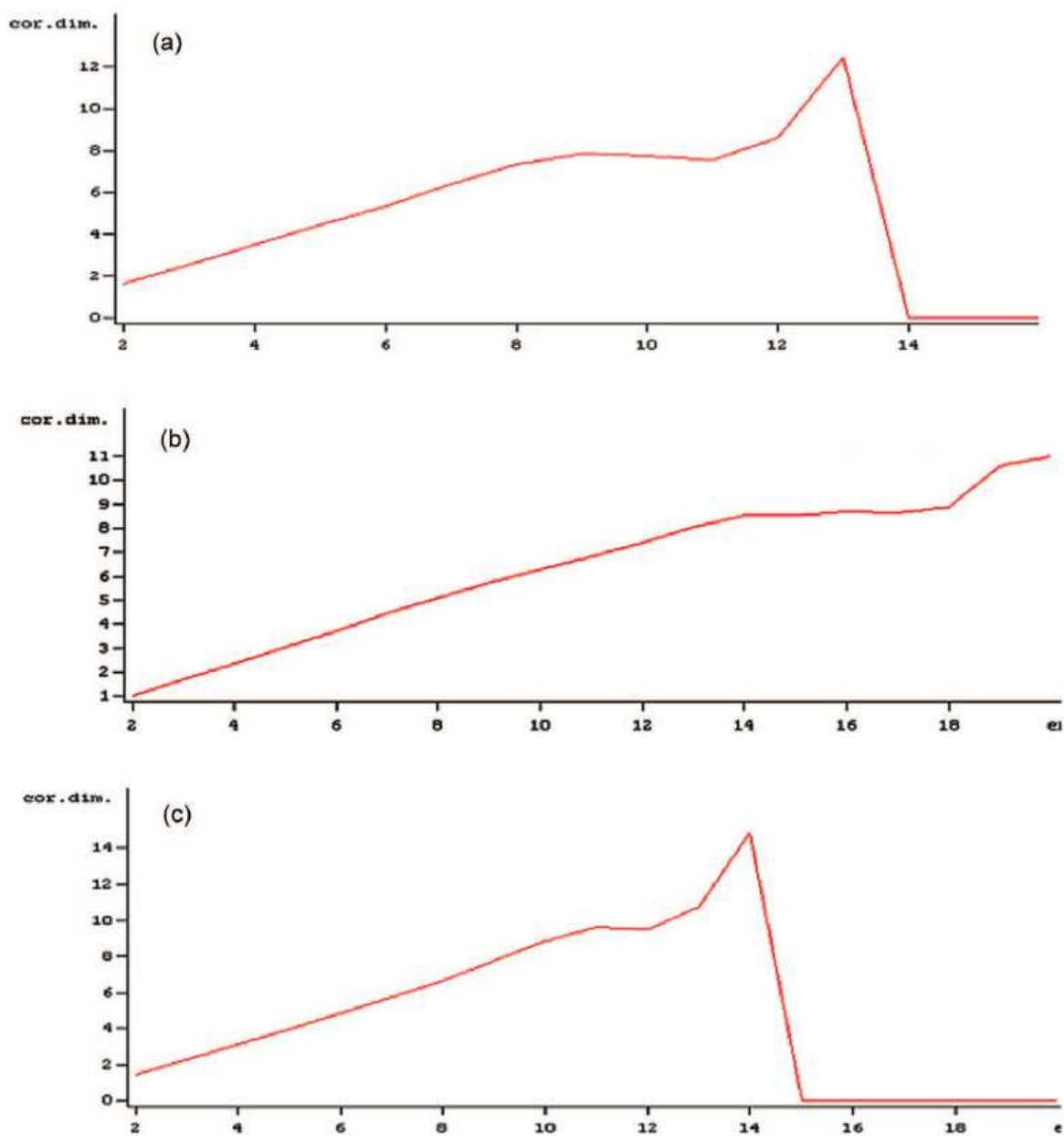


Fig. 4. (a) Graph showing the variations of correlation dimension with embedding dimension for velocity profile. (b) Graph showing the variations of correlation dimension with embedding dimension for density profile. (c) Graph showing the variations of correlation dimension with embedding dimension for temperature profile.

corresponding embedding dimension was 9. A positive value for λ_{\max} which is equal to +0.349 for the velocity data shows chaotic behaviour. The Kolmogorov entropy for this case is 0.37.

Extending this idea of time series analysis to unfiltered density and temperature profiles to calculate the attractor dimensions, for the density profiles the attractor dimension is obtained as 8.54 bits for the embedding dimension 14. The calculated LLE and Kolmogorov entropies are 0.4938 and 0.55. This shows that the density profiles also is chaotic. In the case of temperature profile, the correlation dimension was 9.67 bits for an embedding dimension 11. The LLE and Kolmogorov entropy are 0.403 and 0.47. These results show that it forms another chaotic attractor.

The chaotic behavior is caused by the superposition of more than two modes of oscillation and is due to strong nonlinear coupling between them. At a distance of 1 AU the terrestrial magnetospheric fluctuations give rise to interaction between solar wind particles and the waves associated with them such as low frequency Alfvén waves which leads to nonlinear behavior and chaos.

5. Interaction with Earth's magnetosphere

The Earth has an internal dipole magnetic moment of $8 \times 10^{15} \text{ Tm}^3$ that produces a magnetic field strength at the equator on the Earth's surface of about 30,000 nT, and at 10 Earth radii (R_E) of about 30 nT (Russell, 2000). This dipole moment is created by a magnetic dynamo deep inside the Earth in the fluid, electrically conducting core.

The magnetosphere is the region around a planet that is influenced by that planet's magnetic field. Earth's magnetic field is similar in overall structure to the field of a gigantic bar magnet and completely surrounds our planet. The magnetic field lines, run from south to north. Earth's magnetosphere contains two doughnut-shaped zones of high-energy charged particles, one located about 3000 km and the other 20,000 km above Earth's surface. These zones are named as the Van Allen Belts.

The particles that make up the Van Allen belts originate in the solar wind. When electrically charged particles (mainly electrons and protons) from the solar wind enter into Earth's surface, the magnetic field exerts a force on them and can become trapped by Earth's magnetism causing the particle to spiral around the magnetic field lines and they accumulate into the Van Allen belts.

The positions at which the field lines intersect the atmosphere, particles from the Van Allen belts often escape from the magnetosphere near Earth's north and south magnetic poles. Their collisions with air molecules create a spectacular light show called an aurora. This colorful display results when atmospheric molecules, excited upon collision with the charged particles, fall back to their ground states and emit visible light. Many different colors are produced because each type of atom or molecule can take one of several possible paths as it returns to its ground state. Aurorae are most brilliant at high latitudes, especially inside the Arctic and Antarctic circles. In the north, the spectacle is called the aurora borealis, or Northern Lights. In the south, it is called the aurora australis, or Southern Lights.

The MHD disturbances of three types propagate in this magnetized solar wind plasma. The fast mode wave compresses the magnetic field and plasma; the intermediate mode wave

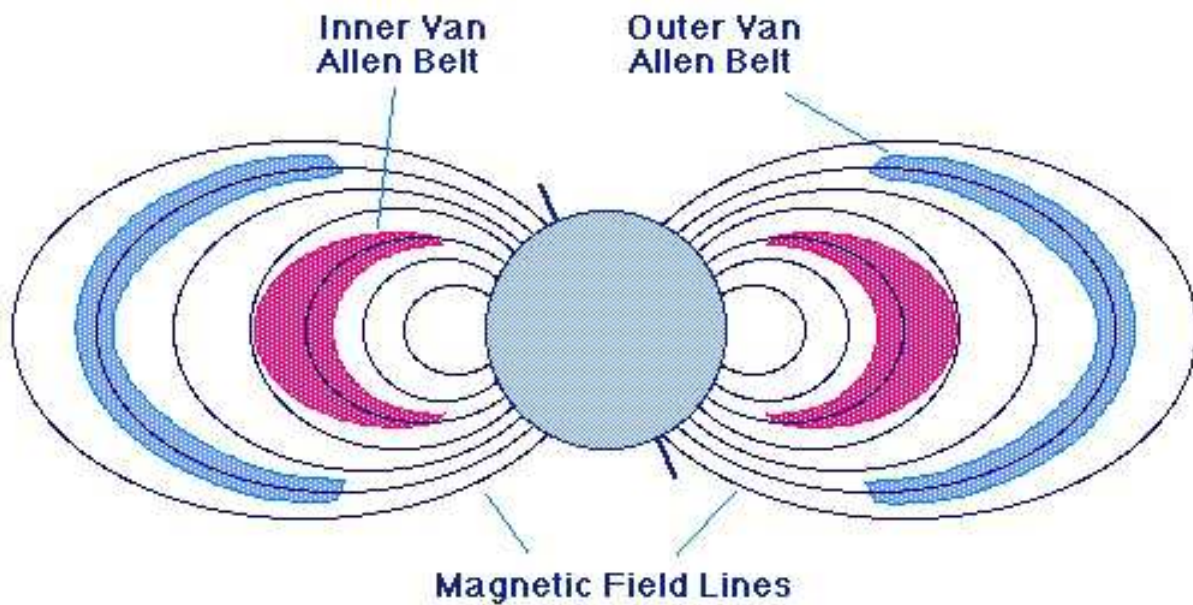


Fig. 5. Van Allen belts

bends the flow and magnetic field, but does not compress it; and the slow mode wave rarefies the field while it compresses the plasma and vice versa.

When the solar wind reaches the earth it causes change in the magnetic field topology, resulting in magnetic merging or magnetic reconnection. Magnetic reconnection at the day side magnetopause is the principal mechanism of energy transfer from the solar wind to the Earth's magnetosphere-this was first proposed by Dungey in 1961. According to Dungey when the frozen-in -condition is relaxed, the field will diffuse relative to the plasma in the magnetopause, allowing the interplanetary and terrestrial field lines to connect through the boundary . This process is termed as magnetic reconnection. The distended loops of open magnetic flux formed by the reconnection exert a magnetic tension force that accelerates the plasma in the boundary north and south away from the site where reconnection takes place, thus causing the open tubes to contract over the magnetopause towards the poles.

The open tubes are then carried downstream by the magneto sheath flow, and stretched in to a long cylindrical tail. Eventually, the open tubes close again by reconnection in the centre of the tail. This process forms distended closed flux tubes on one side of the reconnection cite, which contract back towards the earth and eventually flow to the dayside where the process can repeat. On the other side 'disconnected' field lines accelerate the tail plasma back in to the solar wind.

6. Geomagnetic storms

The Sun is the source of severe space weather. The U. S. National Oceanic and Atmospheric Administration (NOAA), categorizes space weather into three types, which each have their own measurement scales: geomagnetic storms, solar radiation storms, and radio blackouts. Large, violent eruptions of plasma and magnetic fields from the Sun's corona, known as coronal mass ejections (CMEs), are the origin of geomagnetic storms (National Academy of Sciences [NAS], 2008), while solar radiation storms and radio blackouts are caused by solar

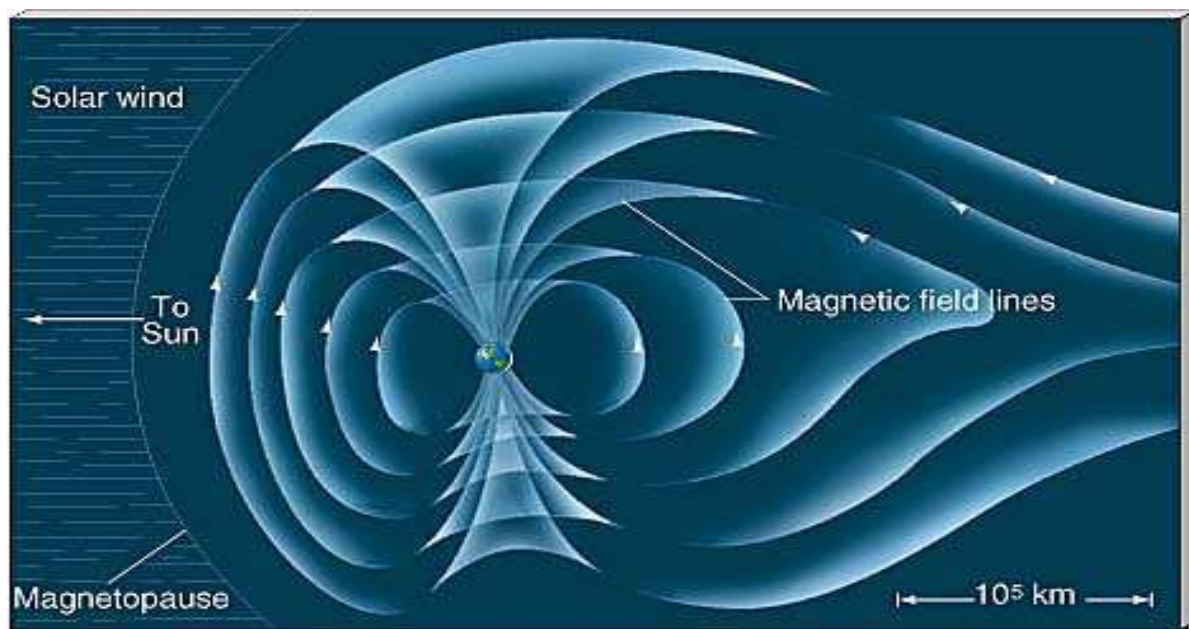


Fig. 6. Distortion in the earth's magnetosphere by the solar wind.

flares. CME shock waves create solar energetic particles (SEPs), which are high-energy particles consisting of electrons and coronal and solar wind ions (mainly protons). When CMEs head towards the Earth, these geomagnetic storms create disturbances that affect the Earth's magnetic field. It takes approximately two to three days after a CME launches from the Sun for a geomagnetic storm to reach Earth and to affect the Earth's geomagnetic field (NERC, 1990).

Geomagnetic storms have the potential to cause damage across the globe with a single event (Schieb, P. A & Gibson, A, 2011). In the past, geomagnetic storms have disrupted space-based assets as well as terrestrial assets such as electric power transmission networks. The TEC of the Earth's ionosphere increases during a geomagnetic storm, which increases the density of the ionosphere and leads to signal propagation delays to and from satellites (Gubbins, et al., 2007). Geomagnetically Induced Currents (GICs) were produced due to the fluctuation in the earth's geomagnetic field caused by the storms. These GICs can flow through power transmission grids (as well as pipelines and undersea cables) and lead to power system problems (Kappenman, 2000). Extra-high-voltage (EHV) transformers and transmission lines—built to increase the reliability of electric power systems in cases of terrestrial hazards—are particularly vulnerable to geomagnetically induced currents (GICs) with recent estimates stating that 300 large EHV transformers would be vulnerable to GICs in the United States (NAS, 2008).

The storm begins when the interplanetary shock wave reached the magnetosphere and compression occurs rather suddenly. After the sudden commencement of the storm there is a period of few hours of calmness. This period is the initial phase. After this the major phase of the storm begins which is called the main phase. The main field strength drops abruptly nearly 50 to 100 gammas below normal. During this period there may be positive and negative fluctuations of short duration. Finally in the recovery phase, the magnetic field strength of the earth returns in a somewhat irregular manner to a quiescent value. The recovery phase requires one or two days provided no other disturbances occur in the mean time.

There are several scales used to measure the severity of geomagnetic storms. The K and A_k indices are used to categorise the intensity of geomagnetic storms. A severe geomagnetic storm is categorized using K values ranging from 7 to 9 and A_k values ranging from 100-400 (Molinski *et al.*, 2000). More severe storms are expressed with higher negative-value D_{st} indices. A severe geomagnetic storm is defined as any event with a D_{st} of less than -500 nanoTeslas (nT). In addition, geomagnetic storm intensity is frequently described in terms of positive nanoTeslas per minute (nTs/min). The 2003 geomagnetic storm 1 peaked at -410 nT. No recorded geomagnetic storm since 1932 has exceeded -760 nT (Cliver and Svalgaard, 2004).

Countries located in northern latitudes, such as Canada, the United States, and the Scandinavian nations, are extremely vulnerable to geomagnetic storms. Power systems located in the northern regions of the North American continent are extremely vulnerable because of their proximity to the Earth's magnetic north pole (Kappenman *et al.*, 1990). Although higher geographic latitudes are more susceptible to geomagnetic storm activity than lower regions, damage from GICs have been witnessed in countries in lower latitudes, such as South Africa (Koen and Guant, no date) and Japan (Thomson, 2009). In addition to mapping out regions based on geological conductivity to predict GIC distribution, a more influential factor on GICs involves changes in the Earth's magnetic field (Thomson, 2009). Together with ground conductivity, these magnetic field changes can generate electric fields which move GICs throughout electrical grids (Kappenman, 2000). GICs also are driven by currents from the earth's magnetosphere and ionosphere.

Because at all latitudes GIC movements are strongly correlated with the rate of change over time of the Earth's magnetic field, the only way to anticipate GIC movements would be to predict magnetic field movements, but predicting changes in the magnetic field is presently very difficult to do (Thomson, 2009). In 2009, twin NASA spacecraft have provided scientists with their first view of the speed, trajectory, and three-dimensional shape of coronal mass ejections, or CMEs. This new capability will dramatically enhance scientists' ability to predict if and how these solar tsunamis could affect Earth.

7. Summary and conclusions

The solar corona consists of tenuous plasma that is highly structured by the strong magnetic field that finds its origin in the solar interior. As the result of varying boundary conditions in the corona, three basic types of solar wind occur: Fast streams from large coronal holes (CHs); slow streams from small CHs and active regions (ARs), and from the boundary layers of coronal streamers; and the variable transient flows such as coronal mass ejections (CMEs). The steady solar wind consists of two major components: fast, tenuous, and uniform flows from large CHs, and slow, dense, and variable flows from small CHs, often from near the boundaries between closed and open coronal fields. The origin of fast streams seems clear, but the sources of the slow solar wind remain less obvious.

The flow of energy through the solar atmosphere and the heating of the Sun's outer regions are still not fully understood. There is no consensus among researchers about the physical mechanism(s) for coronal heating and for solar wind acceleration, even today. The electron driven model is very sensitive to the temperature since the heat flux varies as $T^{7/2}$ but the wind which is the most stable, is the fastest and fills most of the heliosphere, comes from the

coldest regions of the corona. At such a temperature, the thermal conductivity falls short by roughly one order of magnitude of that required to drive even a low-speed wind. Hence the electron driven models were soon recognized to be insufficient to drive the high speed streams.

With heating and wave pressure, the wave-driven models were able to explain the high-speeds and hot protons observed in the fast wind in interplanetary space. These wave-driven models generally succeeded in explaining solar wind data far from the Sun, but they failed close to the Sun. The reason is simply that, close to the Sun, the wave pressure is small compared to other terms in the momentum balance. Because of the perpendicular nature of the heating, and because of the velocity distribution anisotropies for positive ions in the coronal holes, UVCS observations have led to a resurgence of interest in models of coronal ion cyclotron resonance.

Wave-particle interactions, such as ion-cyclotron resonance, are considered now as the principal mechanism for heating of coronal holes, and ultimately driving the fast solar wind. But we still do not know the exact source of the high-frequency resonant waves.

At 1 AU there exists a significant correlation between solar wind velocity with the parameters proton density, proton temperature and average magnetic field in the solar wind. The terrestrial magnetospheric fluctuations give rise to interaction between solar wind particles and the waves associated with them such as low frequency Alfvén waves which lead to nonlinear behavior and chaos at this distance.

When the solar wind reaches the earth it causes change in the magnetic field topology, resulting in magnetic merging or magnetic reconnection. The collision of the CME with the Earth excites a geomagnetic storm. As a natural event whose effect causes economic and technological hazards, geomagnetic storms require both domestic and international policy driven actions.

8. References

- Alazraki, G. , Couturier, P. 1971, *A&A*, 13, 380.
- Alfvén, H. 1942, *Nature*, 150, 405.
- Antonucci, E. , Doderio, M. A. , & Giordano, S. 2000, *Sol. Phys.* , 197, 115.
- Arge, C. N. , Harvey, K. L. , Hudson, H. S. & Kahler, S. W. 2003, in: M. Velli, R. Bruno & F. Malara(eds.), *Solar Wind Ten*, AIP Conf. Proc. , Vol. 679, Melville, New York, USA, p. 202.
- Aschwanden, M.J. (2008), *J. Astrophys. Astr.* 29, 3–16.
- Axford, W. I. , & McKenzie J. F. 1992, in *COSPAR Colloq. 3, Solar Wind* Seven, ed. E. Marsch & R. Schwenn (Oxford: Pergamon).
- Banerjee, D. , Teriaca, L. , Doyle, J. G. 1998, *A&A*, 339, 208.
- Banerjee, D. , Pérez-Suárez, D. , & Doyle, J. G. 2009, *A&A*, 501, L15.
- Barnes, A. , Gazis, P. R. , and Phillips, J. L. ,1995, *Geophys. Res. Letters*. 22, 3309.
- Böhm-Vitense, E. 1989, *Introduction to stellar astrophysics*. Vol. 2, ed.
- Böhm-Vitense, E. (Cambridge: Cambridge University Press).
- Bretherton, F. P. , Garrett, C. J. R. 1969, *Proc. Roy. Soc. A*, 302, 529.
- Burlaga, L. F. , 1991, *Geophys. Res. Lett.* 18, 1651.

- Burlaga, L. F. ,1993, *Astrophys. J.* 407, 347.
- Buti, B. ,1996, *Astrophys. Space Sci.* 243, 33.
- Cowee, M. M. , Winske, D. , Russell, C. T. , & Strangeway, R. J. 2007, *Geophys. Res. Lett.* , 34, L02113.
- Cranmer, S. R. 1999, *ApJ*, 511, 481
- Cranmer, S. R. 2000, *ApJ*, 532, 1197.
- Cranmer, S. R. 2001, *Proceedings of the 14th Topical Conference on Radio Frequency Power in Plasmas*, May 7–9, Oxnard, California, AIP Press.
- Cranmer, S. R. 2002, *Space Sci. Revs.* , 101, 229.
- Cranmer, S. R. 2004, In: *Proceedings of the SOHO 15 Workshop – Coronal Heating* (eds). Walsh, R. W. , Ireland, J. , Danesy, D. , Fleck, B. , European Space Agency, Paris, p. 154.
- Dowdy, J. F. , Jr. , Rabin, D. , & Moore, R. L. ,1986, *Solar Physics*, 105, 35.
- Dungey, J. W. ,1961, *Phys. Rev. Lett.* , 6, 47.
- Dungey, J. W. 1963. , in *Geophysics: The Earth's Environment*, edited by C. Dewitt, J. Hieblot, and A. Lebeau, pp. 505-550, Gordon and Breach, New York.
- De Pontieu, B. 2007, *Science*, 318, 1574.
- Eselevich, V. G. 2009, *Cosmic Research*, , 47, 95–113.
- Gary, S. P. 1991, *Space Sci. Rev.* , 56, 373
- Goodman, M. L. ,2000, *Astrophys. J.* 533, 501–522.
- Guhathakurta, M. , Holzer, T. E. 1994, *ApJ*, 426, 782.
- Guhathakurta, M. , Fisher, R. 1998, *ApJ*, 499, L215.
- Gubbins, David, Emilio Herrero-Bervera, *Encyclopedia of Geomagnetism and Paleomagnetism*, Springer, The Netherlands, 2007.
- Harmon, J. K. , & Coles, W. A. 2005, *J. Geophys. Res.* , 110, A03101.
- Hollweg, J. V. , 1978, *Rev. Geophys. Space Phys.* 16, 689–720.
- Hollweg, J. V. 1986, *J. Geophys. Res.* , 91, 4111.
- Hollweg, J. V. , & Johnson, W. J. 1988, *J. Geophys. Res.* , 93, 9547.
- Hollweg, J. V. 2006, *J. Geophys. Res.* , 111, A12106, doi:10. 1029/2006JA011917.
- Hollweg, J. V. 2008, *JA&A*, 29, 217.
- Huddleston, D. E. , & Johnstone, A. D. 1992, *J. Geophys. Res.* , 97, 12217.
- Jess, D. B. , Mathioudakis, M. , Erd'elyi, R. , Crockett, P. J. , Keenan, F. P. , & Christian, D. J. 2009, *Science*, 323, 1582.
- Jian, K. L. et al. ,(2009). , *Astrophys. J.*, 701, L105.
- John, S. K. , & Kurian, P. J¹. ,2009, *Research in Astron. Astrophys.* , 9, 485.
- John, S. K. , & Kurian, P. J². ,2009, *Pramana*, 72, 743.
- Joseph, L. & P J Kurian (2010) *Journal of Physics: Conference Series* ,208.
- Kappenman, John G. and Vernon D. Albertson (1990), —Bracing for the Geomagnetic Storms: As Solar Activity Moves Toward an 11-Year Peak, Utility Engineers Are Girding for the Effects of Massive Magnetic Disturbances, *IEEE Spectrum* 1990.
- Kappenman, John G. (2000), —Advanced Geomagnetic Storm Forecasting: A Risk Management Tool for Electric Power System Operations, *IEEE Transactions On Plasma Science* 28:6.
- Koen, J. and C. T. Gaunt, *Geomagnetically Induced Currents At Mid-Latitudes*, Department of Electrical Engineering, University of Cape Town, South Africa.
- Kohl, J. L. 1998, *ApJ*, 501, L127.

- Kohl, J. L. 1999, *ApJ*, 510, L59.
- Li, X. , Habbal, S. R. , Kohl, J. L. , & Noci, G. 1998, *ApJ*, 501, L133.
- Liewer, C. P. , Neugebauer, M. & Zurbuchen, T. 2003, in: M. Velli, R. Bruno & F. Malara (eds.), *Solar Wind Ten*, AIP Conf. Proc. , Vol. 679, Melville, New York, USA, p. 51.
- Markovskii, S. A. , 2001, *Astrophys J.* 557:337–342.
- Marsch, E. 1991, in *Physics of Inner Heliosphere*, vol. 2: Particles, Waves, Turbulence, ed. R. Schwenn & E. Marsch (New York: Springer), 45.
- Marsch, E. , 2006, *Origin and evolution of the solar wind*. *Solar Activity and its Magnetic Origin Proceedings IAU Symposium No. 233*, V. Bothmer & A. A. Hady, eds.
- Narain, U. , and Ulmschneider, P. , 1990, *Space Science Reviews* 54, 377.
- NAS (National Academy of Sciences) (2008), *Severe Space Weather Events – Understanding Societal and Economic Impacts Workshop Report*, National Academies Press, Washington, D. C.
- NAS (2009), *Severe Space Weather Events – Understanding Societal and Economic Impacts: A Workshop Report - Extended Summary*, National Academies Press, Washington, D. C.
- NERC (North American Electric Reliability Corporation) (1990), March 13, 1989 *Geomagnetic Disturbance*, NERC, Princeton, NJ.
- Neugebauer, M. 1981, *Fundam. Cosmic Phys.* , 7, 131.
- Neugebauer, M., 1992, in *Solar Wind Seven*, ed. E. Marsch & R. Schwenn (Tarrytown: Pergamon), 69.
- NOAA (National Oceanic and Atmospheric Administration), –Customer Services, National Weather Service Space Weather Prediction Center, <http://www.swpc.noaa.gov/Services/index.html>, accessed 20 September 2010.
- Nolte, J. T. , Kriger, A. S. , Timothy, A. F. , et al. , 1976, *Solar Phys.* , vol. 46, pp. 303.
- Parker, E. N. , 1958, *Astrophys. J.* , 128, 664.
- Parker, E. N. , 1991, *Astrophys. J.* 372, 719.
- Richardson, J. D. 1996, in *Physics of Space Plasmas*, ed. T. Chang & J. R. Jasperse (MIT Space Plasma Group publications).
- Roberts, D. A. , & Miller, J. A. 1998, *Geophys. Res. Lett.* , 25, 607.
- Russell, C. T. , & Blanco-Cano, X. 2007, *J. Atmos. Sol. -Terr. Phys.* , 69, 1723.
- Russell, C. T. , 2000, *Plasma Science*, 28(6), 1818 – 1830.
- Schieb, P. A & Gibson. P. , 2011, OECD/IFP Futures Project on “Future Global Shocks”, CENTRA Technology, Inc. , on behalf of Office of Risk Management and Analysis, United States Department of Homeland Security.
- Thomson, A. W. P. (2009), –Present Day Challenges In Understanding The Geomagnetic Hazard To National Power Grids, *Advances in Space Research* 45.
- Tu, C. -Y. , & Marsch, E. , 1995, *Space Science Reviews* 73, 1–210.
- Tu, C. -Y. , & Marsch, E. 1997, *Sol. Phys.* , 171, 363.
- Tu, C. -Y. , Zhou, C. , Marsch, E. , Xia, L. -D. , Zhao, L. , Wang, J. -X. & Wilhelm, K. 2005, *Science*, 308, 519.
- Tu, C. -Y. , Zhou, C. , Marsch, E. , Wilhelm, K. , Zhao, L. , Xia, L. -D. & Wang, J. -X. 2005, *Astrophys. J.* 624, L133.
- Tomczyk, S. , McIntosh, S. W. , Keil, S. L. et al. 2007, *Science*, 317, 1192.
- Vernet, N. M. , (1999), *Eur. J. Phys.* 20 , 167–176.

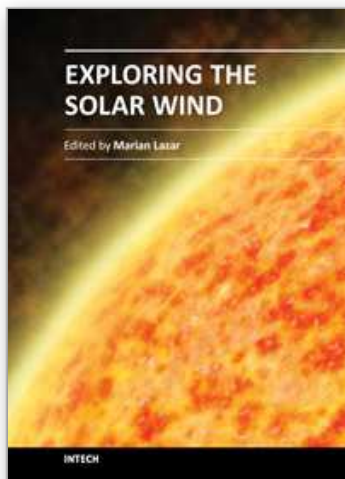
Vidotto, A. A. & Pereira, J. V. , 2009, astro-ph. SR.

Vinas, A. F. , Wong, H. K. , & Klimas, A. J. 2000, ApJ, 528, 509.

Zank, G. P. , Matthaeus, W. H. , Smith, C. W. , and Oughton, S. , 1999, "Heating of the Solar Wind beyond 1 AU by Turbulent Dissipation," in Solar Wind Nine, edited by S. R. Habbal et al. , AIP Conference Proceedings 471, New York, 523.

IntechOpen

IntechOpen



Exploring the Solar Wind

Edited by Dr. Marian Lazar

ISBN 978-953-51-0339-4

Hard cover, 462 pages

Publisher InTech

Published online 21, March, 2012

Published in print edition March, 2012

This book consists of a selection of original papers of the leading scientists in the fields of Space and Planetary Physics, Solar and Space Plasma Physics with important contributions to the theory, modeling and experimental techniques of the solar wind exploration. Its purpose is to provide the means for interested readers to become familiar with the current knowledge of the solar wind formation and elemental composition, the interplanetary dynamical evolution and acceleration of the charged plasma particles, and the guiding magnetic field that connects to the magnetospheric field lines and adjusts the effects of the solar wind on Earth. I am convinced that most of the research scientists actively working in these fields will find in this book many new and interesting ideas.

How to reference

In order to correctly reference this scholarly work, feel free to copy and paste the following:

U.L. Visakh Kumar and P.J. Kurian (2012). Solar Wind: Origin, Properties and Impact on Earth, Exploring the Solar Wind, Dr. Marian Lazar (Ed.), ISBN: 978-953-51-0339-4, InTech, Available from:

<http://www.intechopen.com/books/exploring-the-solar-wind/solar-wind-origin-properties-and-impact-on-earth>

INTech
open science | open minds

InTech Europe

University Campus STeP Ri
Slavka Krautzeka 83/A
51000 Rijeka, Croatia
Phone: +385 (51) 770 447
Fax: +385 (51) 686 166
www.intechopen.com

InTech China

Unit 405, Office Block, Hotel Equatorial Shanghai
No.65, Yan An Road (West), Shanghai, 200040, China
中国上海市延安西路65号上海国际贵都大饭店办公楼405单元
Phone: +86-21-62489820
Fax: +86-21-62489821

© 2012 The Author(s). Licensee IntechOpen. This is an open access article distributed under the terms of the [Creative Commons Attribution 3.0 License](https://creativecommons.org/licenses/by/3.0/), which permits unrestricted use, distribution, and reproduction in any medium, provided the original work is properly cited.

IntechOpen

IntechOpen